BIOCHEMISTRY
including biophysical chemistry & molecular biology

Article

pubs.acs.org/biochemistry

Identification of a Positively Charged Platform in *Staphylococcus aureus* HtsA That Is Essential for Ferric Staphyloferrin A Transport

John D. Cooper,[†] Mélissa Hannauer,[†] Cristina L. Marolda,[†] Lee-Ann K. Briere,[§] and David E. Heinrichs*[,†,‡]

[†]Department of Microbiology and Immunology, [‡]Centre for Human Immunology, and [§]Department of Biochemistry, University of Western Ontario, London, Ontario, Canada

Supporting Information

ABSTRACT: In response to iron starvation, *Staphylococcus aureus* secretes both staphyloferrin A and staphyloferrin B, which are high-affinity iron-chelating molecules. The structures of both HtsA and SirA, the ferric-staphyloferrin A [Fe(III)-SA] and ferric-staphyloferrin B [Fe(III)-SB] receptors, respectively, have recently been determined. The structure of HtsA identifies a novel form of ligand entrapment composed of many positively charged residues. Through ionic interactions, the binding pocket appears highly adapted for the binding of the highly anionic siderophore SA. However, biological validation of the importance of the nine SA-interacting residues (six arginines, one tyrosine, one histidine, and one lysine) has not been previously performed. Here, we mutated each of the Fe(III)-SA-interacting residues in HtsA and found that substitutions R104A, R126A, H209A, R306A, and R306K resulted in a reduction of binding affinity of HtsA for Fe(III)-SA. While mutation of almost all proposed ligand-interacting residues decreased the ability of *S. aureus* cells to transport ^{55}Fe(III)-SA, *S. aureus* expressing HtsA R104A, R126A, R306A, and R306K showed the greatest transport defects and were incapable of growth in iron-restricted growth media in a SA-dependent manner. These three residues cluster together and, relative to other residues in the binding pocket, move very little between the apo and closed holo structures. Their essentiality for receptor function, together with structural information, suggests that they form a positively charged platform that is required for initial contact with the terminal carboxyl groups of the two citrates in the Fe(III)-SA complex. This is a likely mechanism by which HtsA discerns iron-bound SA from iron-free SA.

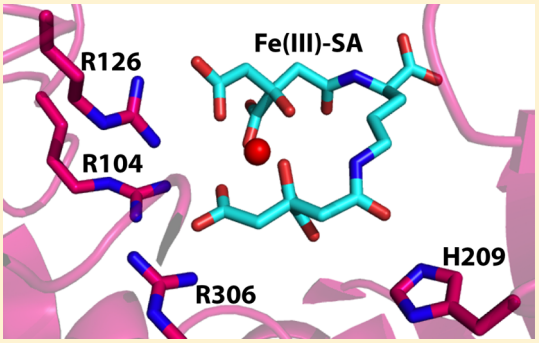

Iron is essential for almost all living organisms, as it participates in many biological processes such as DNA and RNA synthesis, as well as respiration. Despite its high abundance on earth, iron has a low bioavailability at physiological pH. In the human body, due to the sequestration of iron by transferrin or lactoferrin, the concentration of free iron is decreased to 10^{-18} M, whereas bacteria need a concentration of 10^{-6} M for optimal growth.[1,2] Bacterial pathogens have developed many strategies to access sequestered iron, with the most-studied strategy being through the production and use of siderophores, low molecular weight molecules that have high affinity for ferric iron. Siderophores allow growth in low-iron environments by scavenging residual iron found in the environment or growth media, or by stripping iron from transferrin or lactoferrin.

Staphylococcus aureus produces two polycarboxylate-type siderophores: staphyloferrin A (SA) and staphyloferrin B (SB).[3] The proteins encoded by the operon *sbnABCDEFGHI* are responsible for SB biosynthesis[4] and the divergently transcribed *sirABC* genes encode the Fe(III)-SB receptor (SirA; a lipoprotein anchored within the exofacial side of the plasma membrane) and ABC-type transporter permease (SirBC) that are required for Fe-SB uptake into the staphylococcal cell.[3,5,6] SA, composed of D-ornithine and two molecules of citrate, is synthesized by two synthetase enzymes, SfaB and SfaD and PLP-dependent ornithine racemase SfaC.[7] The Fe(III)-SA complex formed extracellularly is transported back into the cell via the HtsABC transporter composed of a lipoprotein receptor (HtsA; a lipoprotein anchored within the exofacial side of the plasma membrane) and a permease (HtsBC).[8] Crystal structures of Fe(III)-SA-bound and unbound forms of HtsA were recently reported and represent the first Gram-positive α-hydroxycarboxylate siderophore receptor structures determined.[9] The structures identify a positively charged binding pocket suitable for the binding of the anionic siderophore SA. Although both SA and SB are anionic α-hydroxycarboxylate siderophores, the receptors for the respective siderophores, HtsA and SirA, are highly specific to their cognate ligand, and the ligand binding pockets share little similarity.[3,6,9]

HtsA is a member of the cluster 8 grouping of periplasmic (in Gram-negative bacteria) or lipoprotein (in Gram-positive

Received: June 11, 2014
Revised: July 19, 2014
Published: July 22, 2014

Table 1. Bacterial Strains and Plasmids Used in This Study

strain/plasmid	genotype/phenotype[a]	source or reference
	S. aureus	
Newman	wild-type clinical isolate	25
RN4220	$r_k^-m_k^+$; accepts foreign DNA	26
H1497	Newman Δ*htABC*::Tc Δ*sirA*::Km; Tc^R Km^R	8
	E. coli	
DH5α	φ_{80} d*LacZ*Δ*M15 recA1 endA1 gyrA9 thi-1 hsdR17*($r_k^-m_k^+$) *supE44 relA1 deoR* Δ(*lacZYA-argF*) *U169*	Promega
ER2566	$F^-\lambda^-$ *fhuA2 [lon] ompT lacZ*::T7 *geneI gal sulA11* Δ(*mcrC-mrr*)114::IS 10 R(*mcr-73*::miniTn*10*)2 R(*zgb-210*::Tn *10*)1 (Tet^S) *endA1* [*dcm*]	New England Biolabs
BL21	F^-, *ompT*, *hsd*S_B (r_B^-, m_B^-), *dcm*, *gal*, λ(DE3), pLysS, Cm^R	Promega
	Plasmids[b]	
pET28a(+)	vector for overexpression of His-tagged proteins using the T7 bacteriophage promoter	Novagen
pEV99	pET28a(+) derivative encoding the soluble portion of HtsA; Km^R	8
pLI50	*E. coli*/*S. aureus* shuttle vector; Ap^R Cm^R	27
pEV55	pLI50 derivative containing *htsABC* from *S. aureus*; Cm^R	8

[a]Abbreviations: Ap^R, Tc^R, Km^R, and Cm^R, resistance to ampicillin, tetracycline, kanamycin, and chloramphenicol, respectively. [b]Shown here are only the template plasmids that were used for cloning and/or mutagenesis. We have not included in the table plasmids expressing mutated HtsA proteins.

bacteria) substrate binding proteins which bind organic metal ion complexes such as Fe(III)-siderophores, heme and cobalamin.[10,11] On the basis of a structure-based classification scheme, these proteins also fall into the type III grouping, comprised of two α/β-domains connected by a long α-helix.[12] The HtsA structure identifies that a novel form of ligand entrapment (i.e., many positively charged residues) is used to bind Fe(III)-SA.[9] K_d values of Fe(III)-SA-HtsA have been determined to be at or below the low nanomolar range. The high affinity of HtsA for its ligand is within the range of several Gram-negative bacterial outer membrane receptors for their respective ligands and is significantly greater than the affinity of *Escherichia coli* FhuD for its ligands. *E. coli* FhuD (ferric hydroxamate uptake protein D) is a periplasmic binding protein that is a receptor for ferric iron complexed with hydroxamate-type siderophores including aerobactin, ferrichrome, desferrioxamine B, and coprogen,[13] and was the first structurally characterized periplasmic binding protein involved in the binding of siderophores.[14] It is not surprising that the affinity of HtsA for Fe(III)-SA is orders of magnitude higher than that of the Gram-negative periplasmic binding proteins, since for these proteins the ligand is concentrated into the periplasm from a much more dilute concentration outside of the cell. The high affinities of HtsA Fe(III)-SA is likely due to the number and type of ionic interactions involved in siderophore coordination. Whereas HtsA is highly specific for Fe(III)-SA, FhuD proteins bind a broad range of Fe(III)-hydroxamate complexes,[13] sacrificing higher affinity for expanded substrate specificity.

The unique open and closed ligand-bound conformations of HtsA allowed identification and characterization of a novel form of ligand entrapment for a type III binding protein. Many crystal structures of related proteins, such as BtuF,[15] TroA,[16] FhuD,[13] and ShuT,[17] have similar overall structural folds but little, if any, conformational changes between apo and holo forms. Although FitE[18] and FeuA[19] both undergo larger hinged movements than HtsA, their conformational changes are characterized by rigid interdomain movement, whereas HtsA conformational changes occur in isolated regions of the C-terminal domain. In addition, the unique HtsA movements help occlude Fe(III)-SA by shifting it deeper in the binding pocket, reducing solvent exposure, and facilitating additional contact points. Compared to other members of this family of binding protein, only SirA has been demonstrated to have similar C-terminal localized domain movements.[6] However, the conformational changes, siderophore orientation, and receptor residues involved in coordination are distinct, and it is not surprising that each receptor is specific for its cognate siderophore.

Given that the *hts*-encoded Fe(III)-SA acquisition system is present ubiquitously among the *Staphylococci*, this system is an ideal candidate for binding affinity and biological studies in order to establish a model system of staphylococcal siderophore uptake. To further characterize the importance of the amino acid residues in Fe(III)-SA binding and transport, we mutated several amino acids in the protein, and the analyses identified four residues, in particular, that were essential for SA-dependent iron acquisition.

MATERIALS AND METHODS

Bacterial Strains and Growth Conditions. The bacterial strains used in this study are described in Table 1. *E. coli* strains were grown in Luria−Bertani broth (LB) in the presence of ampicillin (Ap; 100 μg mL^{-1}) or kanamycin (Km; 40 μg mL^{-1}) for plasmid selection. *S. aureus* strains were grown in tryptic soy broth (TSB) with the following antibiotic concentrations used for selection of strains containing plasmids or chromosomal resistance cassettes: kanamycin, 50 μg mL^{-1}; chloramphenicol, 10 μg mL^{-1}; neomycin, 50 μg mL^{-1}; tetracycline, 4 μg mL^{-1}; erythromycin, 3 μg mL^{-1}. For experiments requiring iron-limiting growth conditions, Tris-minimal succinate (TMS), prepared as described,[20] was used and treated with 10% w/v Chelex 100 resin (Bio-Rad) overnight at 4 °C. All glassware was treated overnight with 0.1 M HCl and rinsed thoroughly with filtered water to remove any residual iron. To further manipulate bioavailable iron, TMS growth media were supplemented with 30 μM $FeCl_3$, 10 μM ethylenediamine-di-*o*-hydroxyphenylacetic acid (EDDHA) (LGC Promochem), or 20% v/v heat-inactivated horse-serum. All solutions and growth media were made with water purified by a Milli-Q purification system (Millipore Corp).

Protein Expression and Purification. The SA synthetases, SfaB and SfaD, and the SA-receptor, HtsA, were purified for use in SA synthesis reactions and Fe-SA fluorescence titration experiments, respectively, as previously described.[9]

dx.doi.org/10.1021/bi500729h | *Biochemistry* 2014, 53, 5060−5069

Table 2. Oligonucleotides Used for Site-Directed Mutagenesis

purpose	sequence[a]
mutation of HtsA, R86K	5′-GTCGATGATGGTAAGAAAAAAAAAATC-3′ (forward)
	5′-CTCTAACTGGTTTAATGATTTTTTTTTTC-3′ (reverse)
mutation of HtsA, R86A	5′-GTCGATGATGGTAAGAAAAAAAAAATC-3′ (forward)
	5′-CTCTAACTGGTTTAATGATTTTTTTTTTC-3′ (reverse)
mutation of HtsA, R104K	5′-GATTATACTTCTGTAGGTACAAAAAAACAGCC-3′ (forward)
	5′-CTTCTAAGTTTGGCTGTTTTTTTGTACCT-3′ (reverse)
mutation of HtsA, R104A	5′-GATTATACTTCTGTAGGTACAGCTAAACAGCC-3′ (forward)
	5′-CTTCTAAGTTTGGCTGTTTAGCTGTACCT-3′ (reverse)
mutation of HtsA, R126K	5′-TCGCTGATAGCAGTAAACATAAAGGTA-3′ (forward)
	5′-CTTTATTAATACCTTTATGTTTACTGCTATCAGC-3′ (reverse)
mutation of HtsA, R126A	5′-GATTTAATTATCGCTGATAGCAGTGCACAT-3′ (forward)
	5′-TATTAATACCTTTATGTGCACTGCTATCAGC-3′ (reverse)
mutation of HtsA, E110A	5′-CCAAACTTAGCAGAAATTAGTAAATTAAAAC-3′ (forward)
	5′-CCGGTTTTAATTTACTAATTTCTGCTAAGTTTG-3′ (reverse)
mutation of HtsA, K203R	5′-CCAGCAGTAGTTGCTAGAGCTGGTT-3′ (forward)
	5′-GATGTGCTAATAAACCAGCTCTAGCAACTA-3′ (reverse)
mutation of HtsA, K203A	5′-CTTCCAGCAGTAGTTGCTGCAGCTG-3′ (forward)
	5′-GATGTGCTAATAAACCAGCTGCAGCA-3′ (reverse)
mutation of HtsA, H209A	5′-GCTAAAGCTGGTTTATTAGCAGCTCCA-3′ (forward)
	5′-GTCCAACATATGAATAGTTTGGAGCTGCT-3′ (reverse)
mutation of HtsA, H209Q	5′-GCTAAAGCTGGTTTATTAGCACAACCA-3′ (forward)
	5′-GTCCAACATATGAATAGTTTGGTTGTGCT-3′ (reverse)
mutation of HtsA, Y239A	5′-CGATGTAACAAAAGGTTTAAGTAAAGCTTTGA-3′ (forward)
	5′-AGTAAGGTCCTTTCAAAGCTTTACTTAAACC-3′ (reverse)
mutation of HtsA, Y239F	5′-CGATGTAACAAAAGGTTTAAGTAAATTTTTGA-3′ (forward)
	5′-AGTAAGGTCCTTTCAAAAATTTACTTAAACC-3′ (reverse)
mutation of HtsA, E250A	5′-CTTACTTACAATTAGACACTGCACATTTAGC-3′ (forward)
	5′-CAGCTAAATGTGCAGTGTCTAATTGTAAG-3′ (reverse)
mutation of HtsA, R299A	5′-GCGTGGATATTGTTGACGCTGATG-3′ (forward)
	5′-AGATCTTGCCCAAACATCAGCGTC-3′ (reverse)
mutation of HtsA, R299K	5′-CGTGGATATTGTTGACAAAAGATGTTTG-3′ (forward)
	5′-CTTGCCCAAACATCTTTGTCAACAATA-3′ (reverse)
mutation of HtsA, R304A	5′-ACCGTGATGTTTGGGCAGCATCT-3′ (forward)
	5′-GAAATTAAGCCACGAGATGCTGCC-3′ (reverse)
mutation of HtsA, R304K	5′-GTGATGTTTGGGCAAAATCTCGTG-3′ (forward)
	5′-ATTAAGCCACGAGATTTTGCCCAAA-5′ (reverse)
mutation of HtsA, R306A	5′-ATGTTTGGGCAAGATCTGCTGGCT-3′ (forward)
	5′-CAGAAGAAATTAAGCCAGCAGATCTTGC-3′ (reverse)
mutation of HtsA, R306K	5′-GATGTTTGGGCAAGATCTAAAGGCTTAAT-3′ (forward)
	5′-CTTCAGAAGAAATTAAGCCTTTAGATCTTGC-3′ (reverse)

[a]Mutated bases are underlined.

Briefly, proteins were expressed and purified from *E. coli* ER2566. Recombinant bacteria were grown at 30 °C in LB (Difco) supplemented with 40 μg mL^{-1} kanamycin. At an OD_{600} of ∼0.9, isopropyl 1-thio-β-D-galactopyranoside (IPTG) (500 μM) was added, and the culture was incubated for an additional 18 h at room temperature with shaking (180 rpm).

Cells were harvested by centrifugation at 15000*g*, resuspended in binding buffer (50 mM HEPES, 500 mM NaCl, 10 mM imidazole at pH 7.4), and lysed with a TS HAIVA cell disruptor (Constant Systems Ltd. UK). Cell lysate was centrifuged at 15000*g* to remove unbroken cells and debris, and the supernatant was centrifuged at 150000*g* for 1 h to precipitate insoluble material. The soluble fraction was filtered with a 0.45um filter and applied to a 1 mL His-Trap nickel affinity column (GE Healthcare) equilibrated with binding buffer (50 mM HEPES, 150 mM NaCl, 10 mM Imidazole, pH 7.4), and His_6-tagged proteins were eluted with a gradient of 0−80% elution buffer (50 mM HEPES, 150 mM NaCl, 500 mM imidazole, pH 7.4). Proteins were then dialyzed into 50 mM HEPES, 150 mM NaCl, and 10% glycerol, pH 7.4, at 4 °C. Protein purity was confirmed using SDS-polyacrylamide gel electrophoresis, and 100 μL aliquots were frozen at −80 °C.

Staphyloferrin A Synthesis and Purification. *In vitro* SA biosynthesis was carried out as previously described, with minor modifications. Briefly, reactions were completed in 500 μL containing 1 mM sodium citrate, 1 mM D-ornithine, 5 mM ATP, 0.5 mM $MgCl_2$, 50 mM HEPES, 5 μM SfaB, and SfaD at pH 7.4, and incubated for 12 h in the dark at room temperature. Following incubation the proteins were removed using a centrifugal filter unit (Amicon Ultra 10K, Merck Millipore Ltd., USA). SA was purified from filtered reactions as described. Fifty to one hundred microliters of the resulting solution was injected onto a Waters xTerra C18 reversed-phase 5-μm column (150 mm × 2.1 mm) on a Beckman System Gold HPLC equipped with a photodiode array detector. The samples were run at 0.2 mL/min using a step gradient as previously

described, with minor modifications. Solvent B was 10 mM tetrabutylammonium phosphate, pH 7.3, in HPLC grade water (Fisher), and solvent A was 100% acetonitrile (Fisher). The step gradient consisted of a 2 min hold at 85% B, a 1 min ramp and 4 min hold at 72% B, a 1 min ramp and 3.5 min hold at 66% B, and a 1 min ramp and 3 min hold at 20% B. Peaks were monitored at 340 nm, and data were analyzed using the 32 Karat Software Version 8.0 system. The peak corresponding to Fe-SA eluted at 17 min and was collected using the Beckman SC 100 fraction collector, vacuum-centrifuged to dryness, and resuspended in deionized water.

Staphyloferrin A Detection and Quantification. The presence of SA following *in vitro* synthesis was confirmed using chrome azurol S (CAS) shuttle solution.[21] Briefly, dilutions of SA reactions were mixed with equal volumes of CAS shuttle solution and incubated for 45 min in the dark at room temperature. SA presence was verified through determination of siderophore units by the following formula: $[(A_{630}$ of control reaction (missing ATP) $- A_{630}$ of sample$)/(A_{630}$ of control reaction$)$(inverse of dilution factor)$] \times 100\%$. The presence of Fe(III)-SA following ion-pair HPLC purification was confirmed using liquid chromatography/mass spectrometry (LC/MS) as previously described, with minor modifications. In brief, EDTA was added to Fe(III)-SA samples to increase SA detection sensitivity in the LC-MS. Atomic absorption spectroscopy was used to indirectly determine the concentration of Fe(III)-SA by measuring the concentration of iron in the HPLC-purified Fe(III)-SA samples, as previously described.[9] Fe(III)-SA samples were diluted in 1 M nitric acid and then drawn by an SPS 5 sample preparation system (autosampler) into a Varian AA240 atomic absorption spectrometer. An iron/manganese hollow cathode lamp was used to detect iron absorbance by emitting at 248.3 nm. Calibration standards were analyzed to generate a linear calibration curve. The curve was generated using known iron standards, diluted in 1 M nitric acid, from an atomic absorption spectrometer certified 1000 ppm ±1% stock (Fisher) before the Fe-SA samples were analyzed.

Site-Directed Mutagenesis. Site-directed mutagenesis was carried out using the QuikChange Site-Directed Mutagenesis Kit (Stratagene), according to the manufacturer's instructions, using plasmids pEV55 and pEV99 as the templates. The oligonucleotides used for the site-specific mutagenesis are listed in Table 2. All mutations were confirmed by DNA sequencing. Mutated plasmids were then used either for testing complementation of a *htsABC* deletion mutant, or for overexpression/purification of HtsA from *E. coli*.

***S. aureus* Whole Cell Lysate Preparation.** *S. aureus* cells were grown overnight in TMS medium, diluted into fresh TMS to an OD_{600} of 0.2, and grown to an OD_{600} of 1.0. 250 μL were harvested via centrifugation (10000*g*), and pellets were resuspended in 50 μL digestion buffer (50 mM Tris pH 7.5, 145 mM NaCl, 10 μM phenylmethylsulfonyl fluoride, 50 μg mL^{-1} lysostaphin (Sigma), 20 μg mL^{-1} DNase) and incubated for 45 min at 37 °C, or until lysis was achieved. Ten microliters were loaded and run through a 12% polyacrylamide gel.

Detergent Partitioning of Membrane Proteins. *S. aureus* cells were grown overnight in TMS medium, diluted into fresh TMS medium, and grown overnight to late-log-phase. The cells were then harvested by centrifugation (10000*g*), washed three times with saline, and equilibrated to an OD_{600} of 1.0 in PBS. The cells were then supplemented with 50 μg mL^{-1} lysostaphin and incubated at 37 °C for 15 min. Detergent extraction and phase partitioning was completed as previously described. Briefly, cells were sonicated using a Branson Digital Sonifier (Branson Ultrasonics Corporation, USA) fitted with a 3 mm-diameter probe, and cooled on ice. 10% v/v Triton X-114 in PBS was then added, and each sample was incubated for 2 h at 4 °C. Samples were then centrifuged (13000*g*) at 4 °C for 10 min to pellet insoluble debris. The supernatants were transferred to clean microcentrifuge tubes, incubated at 37 °C for 30 min, and centrifuged (13000*g*) for 10 min at room temperature. The aqueous phase was then removed, and the pellet was washed with 1 mL PBS at 4 °C for 1 h, transferred to 37 °C for 30 min, pelleted by centrifugation, and resuspended in deionized water.

Generation of Anti-HtsA Antisera. Rabbit polyclonal antibodies recognizing HtsA were generated by ProSci (Poway, CA) using custom antibody production package 1 protocol.

Western Blotting. Following SDS-polyacrylamide electrophoresis, proteins were transferred to a BioTrace NT nitrocellulose membrane (Pall Life Sciences), and blotting was carried out using standard procedures. Primary antiserum was diluted 1:5000, and secondary was used at a 1:7500 dilution. Secondary antibody was goat antirabbit IgG (H&L) conjugated to IRDye800 (Rockland). Membranes were scanned on a Odyssey Infrared Imager (Li-Cor) and visualized using Odyssey V3.0 software (Li-Cor).

Circular Dichroism. Proteins were dialyzed into a solution of 20 mM sodium phosphate, pH 7.4, and 10% glycerol and normalized to a concentration where the A_{280} was ∼0.2. Circular dichroism (CD) spectra were obtained using a J-810 spectropolarimeter (Jasco) with the following settings: standard sensitivity, 260−185 nm measurement range, 0.5 nm data pitch, continuous scanning, 100 nm/min scanning speed, 1 nm bandwidth, and 10 accumulations per sample. Measurements were completed in a 1 mm quartz cuvette, and data were analyzed using Graphpad prism. The CD signal (θ, in millidegrees) was converted to mean residue ellipticity (MRE) ($[\theta]$, in deg·cm^2/dmol) using the equation $[\theta] = \theta \times \mathrm{MRE}/10Cl$, where MRE = MW/n, prior to graphing.

Fluorescence Spectroscopy. Dissociation constants (K_d) for HtsA-Fe(III)-SA complexes were determined using fluorescence spectroscopy as described.[9] In brief, fluorescence titration experiments were performed at room temperature using solution of 15−25 nM HtsA in 50 mM HEPES, pH 7.4, in a Fluorolog-3 spectrofluorometer (ISA Instruments) across a Fe(III)-SA range of 0.22 and 226 nM. Excitation and emission slits were set at 2.1 and 6.3 nm, respectively, and the excitation and emission wavelengths were set at 280 and 334 nm, respectively. K_d values and relevant parameters were calculated by fitting the fluorescence data to a one-site binding model accounting for ligand depletion, and data were analyzed by nonlinear regression.

Growth Assays. Bacteria were cultured for 12 h in TMS broth followed by an additional 12 h in fresh TMS broth. Cells were washed three times with 0.9% w/v saline and diluted 1:100 into 20% horse serum (Sigma-Aldrich) and 80% Chelex 100 resin (Bio-Rad)-treated TMS broth. For iron replete media, 30 μM $FeCl_3$ was added. Cultures were grown with constant, medium amplitude shaking in a Bioscreen C machine (Growth Curves, USA), and optical density was measured at 600 nm every 30 min.

Siderophore Plate-Disk Diffusion Assays. The ability of Fe(III)-SA to promote the iron-restricted growth of *S. aureus* Newman Δ*sirA*Δ*htsABC* harboring plasmid-borne WT or

dx.doi.org/10.1021/bi500729h | *Biochemistry* 2014, 53, 5060−5069

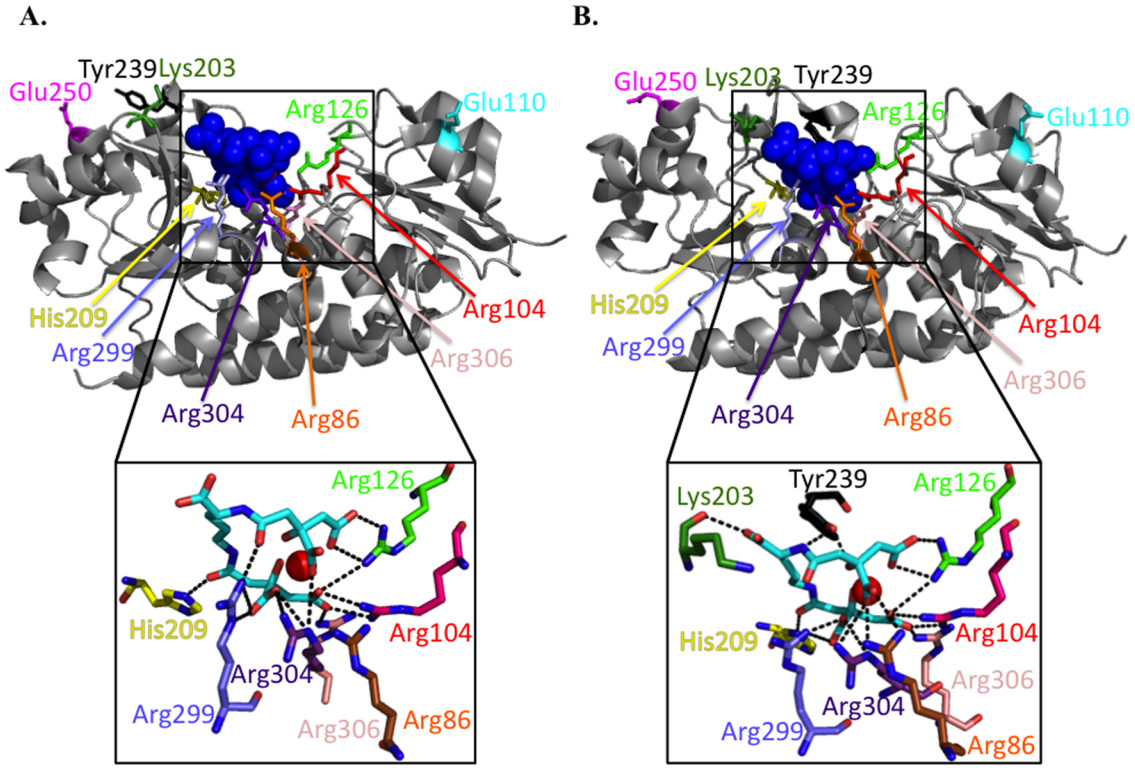

Figure 1. Crystal structure of HtsA open at 1.30 Å (3LHS) (A) and closed at 2.20 Å (3LI2) (B), highlighting the residues that either interact with Fe(III)-SA or the HtsBC permease and which are the focus of this study. HtsA is in gray, staphyloferrin A is in blue and represented in spacefill, and ferric ion is represented by a red ball.

mutant *htsABC* was determined using disk-diffusion assays as previously described,[8] with minor modifications. In brief, *S. aureus* cells were seeded into TMS agar containing 9 μM EDDHA to achieve 1×10^4 cells mL^{-1}. Ten microliters of SA(III)-Fe at 200 μM were added to sterile paper disks, which were then placed onto the plates and incubated at 37 °C. The growth radius was measured after 24 h.

^{55}Fe Transport Assays. $^{55}FeCl_3$ was purchased from PerkinElmer. Potassium cyanide (KCN) was purchased from Fisher Scientific. To prepare the staphyloferrin A-^{55}Fe complex, 200 μM staphyloferrin A is mixed with 20 μM ^{55}Fe. *S. aureus* strains grown overnight in C-TMS were diluted to an OD_{600} of 0.15 in TMS and grown to an approximate OD_{600} of 1. The cells were then harvested by filtration through a 0.45 μm-pore-size membrane filter (Supor-450, Pall Corp.), washed with 10 mL 0.9% NaCl, and resuspended in the same solution to an OD of 1. The suspension is incubated for 15 min at 37 °C before the assay. The transport is started by adding 10 μL of ^{55}Fe-SA to 1 mL of bacterial suspension. After 20 min incubation at 37 °C, 200 μL aliquots were filtered, washed twice with 10 mL of $LiCl_2$, and dried. The radioactivity retained on the filters was counted in scintillation fluid by using the tritium channel of a scintillation system LS6500 (Beckman).

RESULTS

Circular Dichroism (CD) Spectroscopy of HtsA. Our previous studies showed that the HtsABC transporter, along with FhuC ATPase, is required for Fe(III)-SA utilization in *S. aureus*.[8] The HtsA component is anchored to the cytoplasmic membrane by N-terminal acylation and, in this location, serves as a high-affinity receptor for Fe(III)-SA. The *S. aureus* HtsA crystal structure[9] identified that the protein adopts the classical cluster 8 binding protein fold, where two independently folded mixed α/β-domains are separated by a long α-helical backbone (Figure 1). The pocket formed between the lobes represents the Fe(III)-SA binding pocket and, in HtsA, is rich in positively charged side chains that interact with the negatively charged SA molecule that is complexed with an iron atom.

The far UV CD spectrum was used on purified HtsA in order to gain insight into the folding state of the protein in solution. The CD spectrum of HtsA in 20 mM sodium phosphate buffer (pH 7.4), 10% glycerol, after buffer subtraction, showed two negative bands of comparable magnitude centered around 222 and 208 nm, and a strong positive band approaching 190 nm (Figure 2A), features representative of proteins with α-helical structure.[22] The CD data are in agreement with the crystal structure data (from 3EIW, residues 38−327), where it is estimated that 44% of the protein is α-helical, and only 19% β-sheet.

The crystal structures of apo and holo HtsA illustrate that the protein, typical of other representatives of this family of ligand binding proteins, undergoes very little overall conformational change upon ligand binding. Somewhat unique to HtsA, however, are localized loop movements (loops 201−208, 228−258, and 265−271) in transitioning from the apo to holo forms of the protein.[9] In agreement with these data, we observed that the CD spectra of the Fe(III)-SA-bound form of HtsA were identical to the spectra obtained from the apo form of the protein (Figure 2A).

Identification of Substitutions in HtsA that Negatively Impact on Binding to Fe(III)-SA. The cleft formed between the lobes of HtsA represents the Fe(III)-SA binding pocket and, in HtsA, is uniquely rich in positively charged side chains that interact with the negatively charged SA molecule that is

dx.doi.org/10.1021/bi500729h | *Biochemistry* 2014, 53, 5060−5069

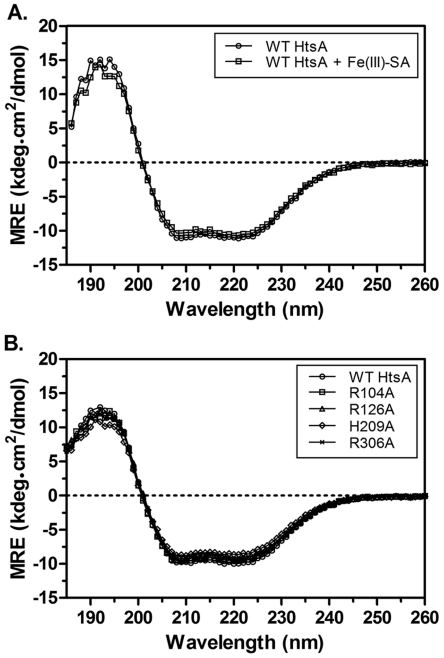

Figure 2. Circular dichroism spectroscopy of purified HtsA and a subset of variants. (A) CD spectra for apoHtsA or HtsA bound to Fe(III)-SA. (B) CD spectra obtained for apoHtsA compared with point mutants as indicated. The mean residue molar ellipticity for each protein is plotted as a function of wavelength. The proteins show strong α-helical signals, which would be predicted based on the structure of the protein.

complexed with an iron atom. To investigate the role of each residue found to interact with SA from crystal structure information, site-directed mutagenesis was performed on pEV99 to substitute residues with either alanine or an amino acid with more conserved properties. In order to confirm that any reductions of the Fe(III)-SA binding affinity caused by mutations in HtsA were not indirectly due to severe alterations in protein secondary structure, CD spectra of each HtsA protein were measured and compared to wild-type HtsA. All spectra (data are shown for only four mutants; see below) were identical to that obtained from wildtype HtsA (see Figure 2B), indicating that none of the mutations that we constructed in HtsA resulted in changes in overall protein structure.

The effect that each mutation had on the Fe(III)-SA-HtsA K_d was determined as described in the Materials and Methods section. It is important to note that an accurate K_d for the HtsA protein could not be determined because it was below the lowest concentration of protein that could be detected in the spectrofluorometer. The K_d of wildtype protein is thus reported here, and elsewhere,[9] to be below the lowest concentration of protein used in the assays (15 nM) (see Table 3). Whereas the majority of the mutant proteins bound Fe(III)-SA similar to wildtype protein, those carrying R104A, R126A, R306A, and R306K mutations resulted in demonstrable increases in K_d, whereas R126K and H209A were moderately impacted for binding (Table 3). For those HtsA mutants whose Fe(III)-SA binding properties were the most altered from wildtype HtsA (i.e. R104K, R126A, R306A, and R306K), we report the CD spectra (Figure 2B) to illustrate that they do not differ from wildtype HtsA in overall secondary structure.

Identification of Substitutions in HtsA That Reduce HtsA-Dependent Growth of *S. aureus* in Iron-Restricted Media.

We next asked whether we could identify mutations that resulted in loss of HtsA function in *S. aureus*. The first assay we chose was one which would differentiate strains expressing mutated HtsA proteins, based on their ability to grow using Fe(III)-SA as a sole source of iron. For this, we used a strain of *S. aureus* (H1497; see Table 1) that is defective in the uptake of both Fe(III)-SA and Fe(III)-SB; this strain demonstrates a drastic reduction of growth in iron-restricted media. The Fe(III)-SA defect is due to a chromosomal deletion of *htsABC*. Beasley et al. demonstrated that the growth of this strain could be rescued via complementation with pEV55, an *E. coli/S. aureus* shuttle vector carrying *S. aureus htsABC*.[8] We performed site-directed mutagenesis on pEV55 to generate the same HtsA substitutions as described above, and the plasmids were then transformed into *S. aureus* H1497. To confirm proper protein expression and localization, Western immunoblots against HtsA were performed on detergent-extracted membrane fractions of *S. aureus* harboring WT or mutant pEV55. None of the mutations constructed affected either the expression level of HtsA or its localization in the membrane (data not shown).

Growth curves of *S. aureus* H1497 harboring either wild-type or mutant derivatives of pEV55 were generated in iron restricted media (Figure 3A–C). While the majority of the binding pocket mutations did not have a demonstrable effect on growth, a drastic growth reduction was observed for strains expressing HtsA with substitutions R104A, R126A, R306A and R306K, while the strain expressing HtsA H209A displayed severely delayed growth. These results are in agreement with the Fe(III)-SA binding affinity data, which indicated that HtsA with substitutions R104A, R126A, H209A, R306A, and R306K had a demonstrable reduction in their ability to bind Fe(III)-SA. All Fe(III)-SA-dependent growth defects were rescued by the addition of 30 μM $FeCl_3$ into the medium (Figure 3D), a growth medium that eliminates the requirement for Fe(III)-SA

Table 3. Dissociation Constants of HtsA and Derivatives for Fe(III)-SA

protein	K_D[a] (nM)
R86A	<15
R86K	<15
R104A	120
R104 K	<15
E110A	<15
R126A	270
R126 K	30
K203A	<15
K203R	<15
H209A	30
H209Q	<15
Y239A	<15
Y239F	<15
E250A	<15
E110A/E250A	<15
R299A	<15
R299K	<15
R304A	<15
R304K	<15
R306A	240
R306K	80

[a]Values are an average of a minimum of three independent experiments.

dx.doi.org/10.1021/bi500729h | *Biochemistry* 2014, 53, 5060–5069

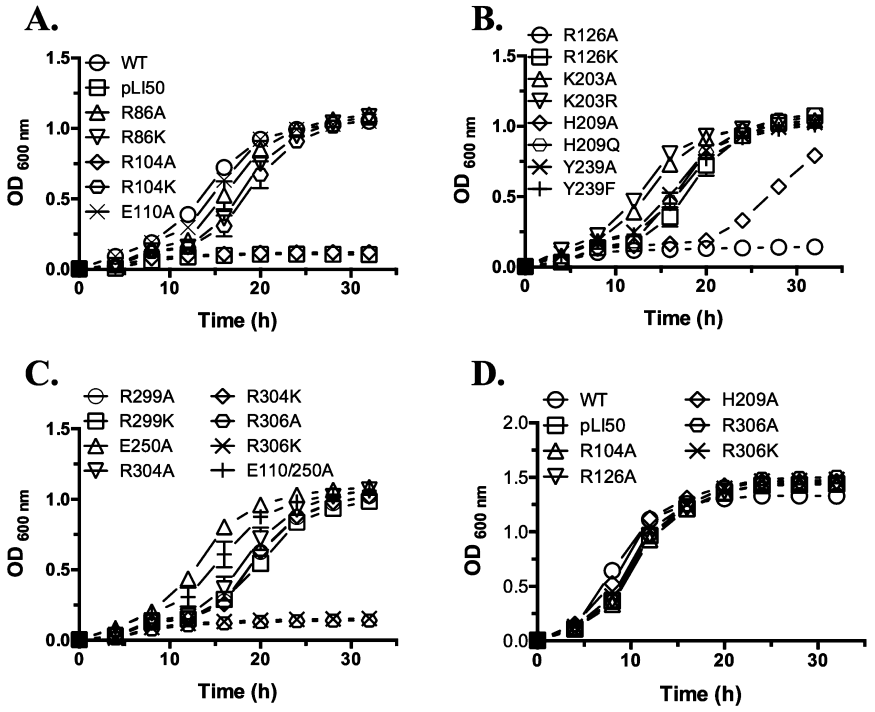

Figure 3. Identification of HtsA mutations that impair Fe(III)-SA-dependent growth of *S. aureus*. *S. aureus* expressing HtsA were grown in C-TMS medium containing 20% serum (A–C). R104A, R126A, H209A, R306A, and R306K mutations impair growth, an impairment that is specific to Fe(III)-SA transport since addition of 30 μM $FeCl_3$ to the growth media bypasses the impairment (D). Error bars represent standard deviation, n = 3.

for growth. These results indicate that no general or pleiotropic growth defects unrelated to Fe(III)-SA uptake were responsible for the observed growth phenotypes.

The growth assay above measured growth dependent upon Fe(III)-SA uptake, reliant on the bacteria to secrete SA into the culture media that could then scavenge available iron and deliver it to be used for growth. However, as our laboratory has previously shown, wildtype-like growth can be achieved in culture media even if an iron transporter is functioning at a level as little as 10% of wildtype.[23] Therefore, we used a second method to assess HtsA transporter function. Siderophore plate bioassays were completed for *S. aureus* H1497 harboring wildtype or mutant pEV55, using purified Fe(III)-SA that was spotted onto the bacteria-containing media. The size of the growth halo around the spotted Fe(III)-SA is a relative measure of its growth promoting ability for each of the strains. As illustrated in Figure 4, growth on Fe(III)-SA for *S. aureus* expressing HtsA R104A, R126A, R306A, or R306K was completely abolished, while it was substantially diminished for the strain expressing HtsA H209A. None of the other substitutions resulted in a significant reduction in the growth radius compared to wildtype. These data correlate well with the liquid culture growth data.

Identification of Substitutions in HtsA That Reduce Fe(III)-SA Uptake. We next wished to directly measure the affect of HtsA mutations on Fe(III)-SA uptake into the *S. aureus* cell. Again, strain H1497 was used but for this assay, we measured ^{55}Fe(III)-SA uptake over a 20 min time period and compared the amount of radioactivity incorporated into the bacteria expressing mutated HtsA protein, in relation to *S. aureus* expressing WT HtsA. To account for signal resulting from nonspecific binding of ^{55}Fe to the cell membranes, controls included wildtype cells treated with KCN prior to

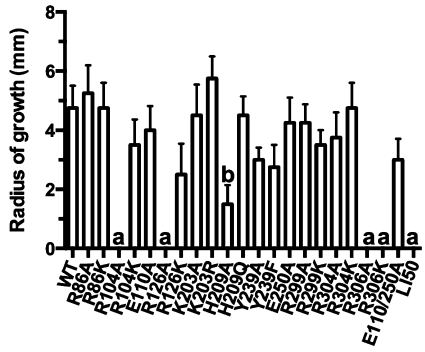

Figure 4. Siderophore plate bioassays identify defects in Fe(III)-SA utilization. *S. aureus* expressing HtsA are seeded in TMS-agar plates and Fe(III)-SA is added as the sole iron source on sterile paper disks. Growth promotion is measured as the radius (mm) of growth around each disk. Error bars represent standard deviation, n = 4. Statistical significance was determined for each mutant in comparison to WT using the Student's unpaired t-test. The symbols "a" and "b" refer to P values $P \leq 0.001$ and $P \leq 0.05$, respectively.

assay (inhibits ATP-dependent transport) and H1497 cells carrying vehicle control (pLI50). As shown in Figure 5, *S. aureus* expressing HtsA substitutions R104A, R126A, R306A, and R306K demonstrated uptake that was less than 10% of *S. aureus* expressing wildtype HtsA. These results correlate well with our preceding data showing that these same substitutions were incapable of supporting Fe(III)-SA dependent growth of *S. aureus*. What is noteworthy about these uptake data, however, is that all substitutions, except for R304 K, result in a decrease in HtsA transporter function relative to wildtype and correlate well with our previous data showing that, for the ferrichrome transporter, even as little as 20% transporter function is enough to support wildtype-like growth under the

dx.doi.org/10.1021/bi500729h | *Biochemistry* 2014, 53, 5060–5069

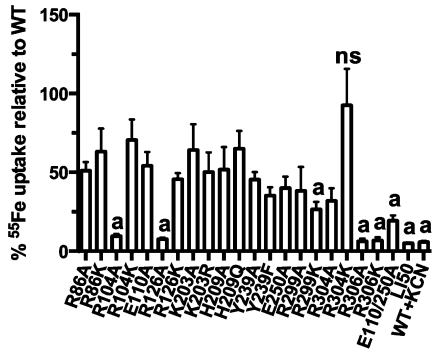

Figure 5. Effects of HtsA mutations on iron acquisition by *S. aureus*. Cells of *S. aureus* expressing HtsA are washed and normalized to an OD_{600} of 1.0. The transport is initiated by adding 100 nM ^{55}Fe(III)-SA. After 20 min incubation, ^{55}Fe incorporation into the cells is measured and compared to wild-type levels. The assay was performed at least 3 times for each strain. Statistical significance was determined for each mutant in comparison to WT using the Student's unpaired *t*-test. The symbol "a" refers to a *P* value of $P \leq 0.001$, and "ns" is not significant. The remainder of the data sets have a *P* value of $P \leq 0.05$.

laboratory growth conditions used. As an example, the E110A E250A double mutant shows only 20% of wildtype transport function over a 20 min period, but the mutant is unaffected in liquid culture growth assays and shows only slightly diminished growth in the siderophore plate bioassay. The E110A E250A substitutions, while not affecting the ability of the protein to bind Fe(III)-SA (see Table 3), likely interfere with the docking of HtsA to the HtsBC permease through salt-bridge interactions. We conclude that the results for the uptake assays are as a consequence of changes in protein function and not differences in protein expression levels, since HtsA variants, especially those with no activity, were expressed in *S. aureus* at equivalent levels (see Figure S1).

DISCUSSION

In this study, we have identified several HtsA residues that are critical for Fe(III)-SA interaction and, thus, HtsA function. The crystal structure of HtsA in complex with Fe(III)-SA identified nine residues that form potential H-bonds with the SA backbone: R86, R104, R126, K203, H209, Y239, R299, R304, and R306. Finally, two residues were identified, E110 and E250, that were predicted to form salt-bridges that mediate docking of HtsA with the permease, HtsBC.

This study identified four residues, in particular, that, when mutated, had the most drastic reductions in Fe(III)-SA binding and that also had a drastic negative impact on the ability of the HtsA protein to function in Fe(III)-SA uptake for iron-restricted growth. Indeed, *S. aureus* expressing any of the HtsA variants R104A, R126A, H209A, R306A, and R306K were the most compromised mutants identified in this study. The importance of these residues is borne out not only by our data here, but also by the fact that, when we analyzed the databases for HtsA orthologs and aligned 140 that shared greater than or equal to 40% identity with the *S. aureus* HtsA sequence from strain USA300, these were four of the most conserved residues (see Table 4). Their overall importance to protein function explains their high degree of conservation. It is interesting to note the importance of the three residues (R104, R126, and R306) that make contact with the terminal carboxyl groups of the citrates in SA. Noteworthy is that substitution of arginine for a lysine at positions 104 and 126 resulted in retained protein

Table 4. Conservation of Residues within HtsA Orthologs

residue	#identical/#total[a]	% ID
	SA Interacting	
R86	92/140	65
R104	140/140	100
R126	137/140[b]	98[b]
K203	85/140	61
H209	134/140	96
Y239	101/140	72
R299	140/140	100
R304	113/140	81
R306	140/140	100
	HtsBC Iinteracting	
E110	133/140	95
E250	132/140	94

[a]Genomes were scanned for HtsA homologous sequences with amino acid sequence identity greater than 40%. Organisms from which HtsA orthologs, and that are included in this table, were identified are as follows: *S. aureus, S. capitis, S. epidermidis, S. lugdunensis, S. pasteuri, S. warneri, S. homini, S. hemolyticus, S. caprae, S. simiae, S. saprophyticus, S. xylosus, S. simulans, S. equorum, S. intermedius, S. pseudintermedius, S. carnosus, S. delphini, S. massiliensis, S. petterkoferi, S. lentus, Bacillus cereus, B. megaterium, B. endophyticus, B. mojavensis, B. tequilensis, B. subtilis, B. vallismortis, B. sonorensis, B. atrophaeus, Viridibacillus arenosi, Paenibacillus alvei, P. mucilaginosus, Salimicrobium* MJ3. [b]Of the three Arg that are not identical, the residue is Lys.

function, whereas the same Arg to Lys substitution at position 306, making contact with the more buried of the two citrates, was not tolerated. These three residues cluster together in the HtsA structure and demonstrate negligible movement upon ligand binding (see Figure 6). We suggest that these three residues thus form a positively charged platform that is essential for the initial interaction between HtsA and Fe(III)-SA. That this platform interacts with both of the terminal citrate carboxyls that are interacting with the iron atom suggests that this platform favors an interaction with SA only when SA is bound to iron.

Histidine at position 209, which makes contact with the carbonyl group of the more buried citrate, is also a highly conserved position among HtsA proteins. Noteworthy is that while its substitution to alanine negatively impacted the K_d and reduced HtsA function, a glutamine in that position re-established low nanomolar binding affinity and partially rescued protein function, indicating the importance of a nitrogen at this position for H-bonding to this carbonyl group. H209A has decreased affinity for Fe(III)-SA and has partial activity based on our other assays for its function (see Figures 4 and 5). Expression of H209A in *S. aureus* results in delayed growth in Fe(III)-SA-dependent iron restricted media (Figure 3), and we suggest that our data support that the hypothesis that this growth delay is due to the requirement for SA to build up in the culture media to a higher concentration, compared to WT HtsA, before it begins to bind Fe(III)-SA in the medium. Once beyond a threshold concentration, the H209A HtsA variant will transport Fe(III)-SA and allow growth.

As expected, substitution of HtsA E110A and E250A, positions that are located outside of the binding pocket and predicted to be involved in docking with HtsBC, did not change the apparent binding affinity of the protein but decreased protein function as determined by the radioactive uptake assays used in this study. Indeed, HtsA E110 and E250 are both highly conserved among HtsA orthologs (see Table 4)

dx.doi.org/10.1021/bi500729h | *Biochemistry* 2014, 53, 5060−5069

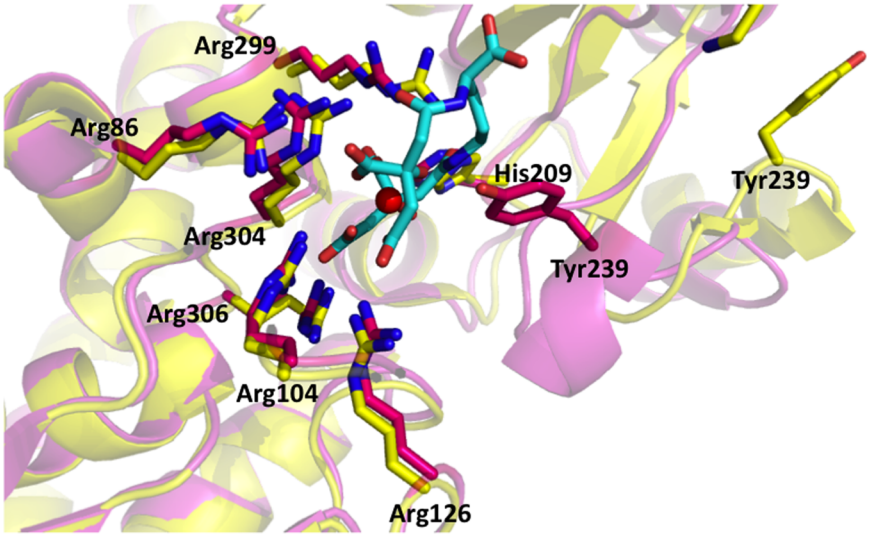

Figure 6. Identification of an essential, positively charged platform in HtsA for interaction with Fe(III)-SA. An overlay of HtsA in the apo (yellow) and Fe(III)-SA-bound (pink) forms shows, of the residues that interact with Fe(III)-SA, R104, R126, and R306 form a cluster of positive charge that interacts with the terminal carboxyls on the two citrates in SA. It is hypothesized that the essentiality of these three residues, in particular, is borne out by their role in the initial capture of Fe(III)-SA by HtsA. The Fe(III) ion is shown as a red sphere.

and glutamic acid residues at these positions in the two lobes are highly conserved in all members of the cluster 8 binding proteins. Modeling of HtsBC with the Fe(III)-SA-HtsA crystal structure predicted that they are involved in Glu-Arg salt-bridge formation between the receptor and membrane transporter. Importantly, similar salt-bridge formation and subsequent docking with their cognate ABC-transporter is necessary for productive transport in related proteins, including *E. coli* FecB[24] and *S. aureus* FhuD2.[23] As mentioned above, our data highlight that while HtsA E110A E250A is not impaired for ligand binding, it is impaired for Fe(III)-SA uptake as determined by our radioactive uptake assays. Our biological assays, such as growth in the presence of the Fe(III)-SA complex were not so definitive and show no debilitation of the mutant, relative to the wildtype, for iron-restricted growth. Together, these data highlight the caution that should be taken in drawing conclusions from bacterial growth assays without having used multiple biological and/or biochemical assays to assess protein function.

It is interesting to note that K203 and Y239 are both involved in H-bonding with Fe(III)-SA in the closed conformation based on the localized movement of a C-terminal loop that moves upon ligand binding to enclose the Fe(III)-SA complex into the binding pocket. However, substitution of either residue to Ala appeared not to have a major impact on protein function. In accordance with this finding, we note that these two positions are two of the least well-conserved residues among HtsA orthologs (Table 4). The biological significance of the localized loop movements involving K203 and Y239 remains to be defined.

CONCLUSIONS

In this study, we used several complementary techniques to identify residues that are required for the binding and transport of ferric staphyloferrin A by its receptor protein, HtsA. Four of the most conserved residues within the binding pocket of HtsA orthologs, R104, R126, H209, and R306, have all been identified in this study as crucial for Fe(III)-SA binding and, thus, protein function. This study confirms the importance of the overall positive character of the HtsA binding pocket for recognition and transport of the anionic ferric staphyloferrin A complex.

ASSOCIATED CONTENT

Supporting Information

Figure S1. HtsA variants expressed at equivalent levels in *S. aureus*. This material is available free of charge via the Internet at http://pubs.acs.org.

AUTHOR INFORMATION

Corresponding Author

*E-mail: deh@uwo.ca. Phone: (519) 661-3984. Fax: (519) 661-3499.

Funding

This project was funded by Grant MOP-38002 to D.E.H. from the Canadian Institutes of Health Research.

Notes

The authors declare no competing financial interest.

ACKNOWLEDGMENTS

We thank Dr. Michael E. P. Murphy, from the University of British Columbia, for stimulating scientific discussions and for critically reading the manuscript.

REFERENCES

(1) Bullen, J. J. (1981) The significance of iron in infection. *Rev. Infect. Dis. 3*, 1127−1138.

(2) Ratledge, C., and Dover, L. G. (2000) Iron metabolism in pathogenic bacteria. *Annu. Rev. Microbiol. 54*, 881−941.

(3) Beasley, F. C., and Heinrichs, D. E. (2010) Siderophore-mediated iron acquisition in the staphylococci. *J. Inorg. Biochem 104*, 282−288.

(4) Cheung, J., Beasley, F. C., Liu, S., Lajoie, G. A., and Heinrichs, D. E. (2009) Molecular characterization of staphyloferrin B biosynthesis in *Staphylococcus aureus*. *Mol. Microbiol. 74*, 594−608.

(5) Dale, S. E., Sebulsky, M. T., and Heinrichs, D. E. (2004) Involvement of SirABC in iron-siderophore import in Staphylococcus aureus. *J. Bacteriol. 186*, 8356−8362.

(6) Grigg, J. C., Cheung, J., Heinrichs, D. E., and Murphy, M. E. P. (2010) Specificity of Staphyloferrin B recognition by the SirA receptor from *Staphylococcus aureus*. *J. Biol. Chem. 285*, 34579−34588.
(7) Cotton, J. L., Tao, J., and Balibar, C. J. (2009) Identification and characterization of the *Staphylococcus aureus* gene cluster coding for staphyloferrin A. *Biochemistry 48*, 1025−35.
(8) Beasley, F. C., Vinés, E. D., Grigg, J. C., Zheng, Q., Liu, S., Lajoie, G. A., Murphy, M. E. P., and Heinrichs, D. E. (2009) Characterization of staphyloferrin A biosynthetic and transport mutants in *Staphylococcus aureus*. *Mol. Microbiol. 72*, 947−963.
(9) Grigg, J. C., Cooper, J. D., Cheung, J., Heinrichs, D. E., and Murphy, M. E. (2010) The *Staphylococcus aureus* siderophore receptor HtsA undergoes localized conformational changes to enclose staphyloferrin A in an arginine-rich binding pocket. *J. Biol. Chem. 285*, 11162−71.
(10) Tam, R., and Saier, M. H. (1993) Structural, functional, and evolutionary relationships among extracellular solute-binding receptors of bacteria. *Microbiol. Rev. 57*, 320−346.
(11) Krewulak, K. D., and Vogel, H. J. (2008) Structural biology of bacterial iron uptake. *Biochim. Biophys. Acta 1778*, 1781−1804.
(12) Chu, B. C. H., and Vogel, H. J. (2011) A structural and functional analysis of type III periplasmic and substrate binding proteins: their role in bacterial siderophore and heme transport. *Biol. Chem. 392*, 39−52.
(13) Clarke, T. E., Braun, V., Winkelmann, G., Tari, L. W., and Vogel, H. J. (2002) X-ray crystallographic structures of the Escherichia coli periplasmic protein FhuD bound to hydroxamate-type siderophores and the antibiotic albomycin. *J. Biol. Chem. 277*, 13966−72.
(14) Clarke, T. E., Ku, S. Y., Dougan, D. R., Vogel, H. J., and Tari, L. W. (2000) The structure of the ferric siderophore binding protein FhuD complexed with gallichrome. *Nat. Struct. Biol. 7*, 287−291.
(15) Karpowich, N. K., Huang, H. H., Smith, P. C., and Hunt, J. F. (2003) Crystal Structures of the BtuF Periplasmic-binding Protein for Vitamin B12 Suggest a Functionally Important Reduction in Protein Mobility upon Ligand Binding. *J. Biol. Chem. 278*, 8429−34.
(16) Lee, Y. H., Dorwart, M. R., Hazlett, K. R., Deka, R. K., Norgard, M. V., Radolf, J. D., and Hasemann, C. A. (2002) The crystal structure of Zn(II)-free Treponema pallidum TroA, a periplasmic metal-binding protein, reveals a closed conformation. *J. Bacteriol. 184*, 2300−4.
(17) Eakanunkul, S., Lukat-Rodgers, G. S., Sumithran, S., Ghosh, A., Rodgers, K. R., Dawson, J. H., and Wilks, A. (2005) Characterization of the periplasmic heme-binding protein ShuT from the heme uptake system of Shigella dysenteriae. *Biochemistry 44*, 13179−91.
(18) Shi, R., Proteau, A., Wagner, J., Cui, Q., Purisima, E. O., Matte, A., and Cygler, M. (2009) Trapping open and closed forms of FitE: a group III periplasmic binding protein. *Proteins 75*, 598−609.
(19) Peuckert, F., Miethke, M., Albrecht, A. G., Essen, L.-O., and Marahiel, M. A. (2009) Structural basis and stereochemistry of triscatecholate siderophore binding by FeuA. *Angew. Chem., Int. Ed. Engl. 48*, 7924−7927.
(20) Sebulsky, M. T., Speziali, C. D., Shilton, B. H., Edgell, D. R., and Heinrichs, D. E. (2004) FhuD1, a ferric hydroxamate-binding lipoprotein in Staphylococcus aureus: a case of gene duplication and lateral transfer. *J. Biol. Chem. 279*, 53152−9.
(21) Schwyn, B., and Neilands, J. B. (1987) Universal chemical assay for the detection and determination of siderophores. *Anal. Biochem. 160*, 47−56.
(22) Woody, R. W. (1995) Circular dichroism. *Methods Enzymol. 246*, 34−71.
(23) Vinés, E. D., Speziali, C. D., and Heinrichs, D. E. (2014) Demonstration of the functional role of conserved Glu-Arg residues in the *Staphylococcus aureus* ferrichrome transporter. *Biometals 27*, 143−153.
(24) Braun, V., and Herrmann, C. (2007) Docking of the periplasmic FecB binding protein to the FecCD transmembrane proteins in the ferric citrate transport system of *Escherichia coli*. *J. Bacteriol. 189*, 6913−8.
(25) Duthie, E. S., and Lorenz, L. L. (1952) Staphylococcal coagulase; mode of action and antigenicity. *J. Gen. Microbiol. 6*, 95−107.
(26) Kreiswirth, B. N., Löfdahl, S., Betley, M. J., O'Reilly, M., Schlievert, P. M., Bergdoll, M. S., and Novick, R. P. (1983) The toxic shock syndrome exotoxin structural gene is not detectably transmitted by a prophage. *Nature 305*, 709−712.
(27) Lee, C. Y., and Iandolo, J. J. (1986) Lysogenic conversion of staphylococcal lipase is caused by insertion of the bacteriophage L54a genome into the lipase structural gene. *J. Bacteriol. 166*, 385−391.